BULLETIN OF BIOTECHNOLOGY

BULLETIN OF BIOTECHNOLOGY

Contents

Bulletin of Biotechnology

Crystal violet removal study with natural and biochar prina from aqueous solutions

Sevda Esma Darama[1*] , Özlem Uçar[1], Semra Çoruh[1]

[*1]Environmental Engineering Department, Engineering Faculty, Ondokuz Mayıs University, Samsun, Turkey.

Abstract: In this study, as industrial waste, prina was used as an adsorbent substance with its natural and thermally modified form. The prina used in the study was taken as waste material from an olive oil factory in Ayvalık, Turkey. In this study, the removal possibilities of the toxic effect of crystal violet dye found in various industrial wastewaters with prina adsorbent were investigated. By using the pyrolysis method at 600 °C, the biochar form of prina was obtained. Natural and biochar prina and crystal violet (CV) dye have been tried under different adsorption conditions. For this purpose, experiments were carried out at different prina dosages, initial dye concentrations and contact times. The highest removal efficiencies are around 75% in natural prina, while the biochar is around 99% in prina. Also, concentration studies were applied to Langmuir and Freundlich adsorption isotherm models. As a result of the isotherm study, it was seen that the adsorption mechanism was suitable for Freundlich isotherm model. The contact time removal studies were applied to pseudo-first-order, pseudo-second-order and intraparticle diffusion kinetic models, and adsorption was found to be fit with the pseudo-second-order kinetic model. According to the experiment results, it was observed that the thermal treatment caused a significant increase in the removal efficiency. It was found that it is an efficient adsorbent material that can be used to remove the CV dye from the aqueous solutions.

Keywords: Adsorption; biochar; crystal violet; dye removal; isotherms; kinetics.

1 Introduction

Olive and oil industry have great economic importance in many Mediterranean countries. According to the Olive And Olive Oil Report For 2018 has approximately 95 million olive trees and 658 000 hectares of olive groves in Turkey and 100.000-250.000 tons of annual oil production in Turkey (T.C. Ministry of Commerce 2019). Olive oil is produced from olives using hydraulic presses or modern horizontal axis centrifuges, and both processes produce highly polluted wastewater and or solid waste. Solid wastes are generally known as "olive cake" or "olive rice". The olive waste consists of cellulose, lignin, amino acid, protein and uronic acids, and oily waste and polyphenolic compounds. These components contain many functional groups. These include carboxylic, hydroxylic and methoxy groups, and many of fixed anionic and cationic functional groups. Prina is usually swallowed through controlled spreading to agricultural soil. Only a small amount of this sediment is used as a natural fertilizer in animal foods, a heat energy source and additives. It is not believed that most of these applications have significant economic value. It is, therefore, useful to find other applications for such an agro-industrial solid waste. (Akar et al. 2009)

Prina, obtained from olive oil factories, is an agricultural product produced in Mediterranean countries. It is exposed during the extraction of olive oil. Make up 6-8% residual olives, 20-33% water, 59-74% seed. Olive oil factories produce about 15-22 kg of olive oil and 35-45 kg of prina from 100 kg of olives in olive oil extraction processes. There are many studies on pollutant removal from wastewater with prina. (Malkoç et al. 2006)

Crystal Violet is an inexpensive dyestuff used for silk, leather, paper dyeing and many different purposes. Besides, culture staining is also frequently used in microbiology. It has a very dense and sticky dye. When the crystal violet dissolves in water, it significantly reduces the light transmittance and disrupts the natural ecolgical balance. Crystal violet is a tri-phenylmethane dye. Crystal violet dye is a water-soluble, toxic organic paint that causes serious health problems and environmental pollution (Cheruiyot et al. 2019).

In general, the dyes are divided into three classes: cationic or basic dyes, anionic or acidic and nonionic or disperse dyes. Cationic dyes, in particular, are primarily applied in the textile industry as water-soluble, cost-effective and widely distributed in the relevant market. Synthetic origins and

aromatic structure dye molecules are generally very stable and cannot be eliminated in nature; also, they are often toxic and suspected to be carcinogenic. It is, therefore, interesting to remove dyes from industrial wastewater. Even though many different physical, chemical, electrochemical and biological methods have been proposed to remove dyes from polluted waters, adsorption has significant advantages over them due to good efficiency, versatility and relatively low costs for removing organic substances well as considerable flexibility against high pollutant load. (Toumi et al. 2018).

The adsorption process takes place in the presence of an adsorbent layer that binds the molecules through physical forces, ion exchange and chemical forces. Adsorption is a treatment process that removes all dye molecules and leaves no parts in wastewater (Rangabhashiyam et al. 2013).

In this study, prina was used in the color removal of crystal violet dye prepared in the laboratory. The availability of the prina in waste status in terms of pollution removal has been investigated and it has been emphasized that it can be a valuable and inexpensive substance.
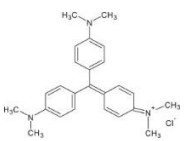
2 Materials and Method

2.1 Materials

The prina used in this study was obtained from an olive oil factory in Ayvalık, Turkey. The prina was washed three times with distilled water. The washed prina was dried in a 103 °C oven for 24 hours. The dried prina was crushed with a Waring brand blender and sieved at 30 mesh. This 30 mesh prina was used as a natural adsorbent.

For the preparation of biochar prina adsorbent, 30 mesh natural prina was operationalised to pyrolysis. Biochar production was carried out with a Uniterm brand high-temperature reactor. The reactor provides a stable temperature through mantle heating. The reactor chamber consists of titanium alloyed stainless steel material. There are inlet and outlet section that provides nitrogen gas flow in the reactor. The gas outlet part was passed through ice water and cooled. The pyrolysis process was carried out at a slow pyrolysis rate of 5 °C/min at 600 temperature, under 100 mL/min nitrogen gas flow, 1 hour waiting time conditions. Pyrolysis conditions were determined by testing similar pyrolysis studies in the literature and selecting average values (Qiu et al. 2018; Demiral and Şamdan 2016; Georgieva et al. 2020; Kaya et al. 2020). 6.38 g biochar was obtained from 20 g of raw prina placed in the steel reactor. The obtained biochar is ready for use in the experiment as adsorbent.

Table 1 Some properties of crystal violet dye

CAS No.	Chemical	Molecular Weight	C.I. Name	Molecular Structure
548-62-9	$C_{25}H_{30}ClN_3$	407.979 g/mol	Basic Dye	

Crystal violet ($C_{25}H_{30}ClN_3$) was chosen for adsorption studies. The wastewater sample was prepared as a synthetic aqueous solution with a concentration of 1000 mg/L with CV solid dye. 1000 mg/L stock solution was prepared by dissolving correctly weighed amounts of CV in 1000 mL distilled water. Table 1 shows some of the properties of CV dye.

2.1 Method

Adsorption studies were carried out with natural and biochar prina under different adsorption conditions to reduce the CV concentration. Adsorption experiments run to determine maximum removal conditions; at different prina dosages (2-4-8-20 g/L), at contact times (1-15-30-60-90-120-240 min) and initial CV concentration (50-100-200-400-600-800 mg/L). General adsorption conditions were carried out at 25 mL CV solution volume, 8 g/L walnut shell dosage, 50 mg/L initial CV concentration and 60 min contact time.

The prepared solutions were mixed with an Innova model 2000 brand platform shaker at 175 rpm for 60 minutes. After mixing, samples were centrifuged at 9000 rpm for 10 minutes then, after adsorption, CV concentrations were measured with a Thermo brand Aquamate model UV spectrophotometer at 590 nm wavelength.

Also, the initial concentration study was applied to adsorption Langmuir and Freundlich isotherm models. The contact time study was applied to pseudo-first-order, pseudo-second-order model and intra-particle diffusion kinetic models.

Removal efficiency values after adsorption calculated by Equation 1;

$$E(\%) = \frac{C_0 - C_e}{C_0} \times 100 \qquad (1)$$

There; E (%) is percent removal efficiency, C_0 (mg/L) initial CV concentration, and C_e (mg/L) CV concentration after adsorption.

Also, adsorption capacities were calculated in all adsorption studies. Adsorption capacity is the amount of adsorbate that the adsorbent's unit mass (or volume) can adsorb. The adsorption capacity (qe) is formulated in Equation 2;

$$q_e(mg/g) = \frac{C_0 - C_e}{m} \times V \qquad (2)$$

Where; C_0 and C_e (mg/L) are the initial concentration and equilibrium concentration of dye solution, respectively, V (L) is the volume of dye solution and m (g) is the mass of adsorbent.

3 Results and Discussion

3.1 Effect of adsorbent dosage on removal

To determine the optimum dosage, natural and biochar prina was subjected to adsorption process at 2-4-8-20 g/L adsorbent dosages, 25 mL sample volume, 50 mg/L initial CV concentration for 60 minutes contact time. Removal

efficiencies and adsorption capacity (qe) values were calculated for natural and biochar prina.

The results of the dosage study are given in Figure 1. In general, removal efficiency also increased with increasing dosage of adsorbents. However, removal efficiencies at 8 g/L and 20 g/L are very close to each other, therefore 8 g/L was chosen as the optimum adsorption dosage. Looking at the graph, biochar prina has 20-25% higher removal efficiency compared to natural prina. The selected dosage is at 8 g/L, the yields are 75.85% and 98.14% for natural and biochar prina, respectively. With increasing adsorbent dosage, removal efficiency has also increased. The yields started to stabilize after the 8 g/L dosage. This is due to the increase in the available surface area and the number of adsorption areas. The higher the adsorbent dosage, the more binding area is available for the CV to be taken up to the prina surface. The selected dosage is at 8 g/L, the yields are 75.85% and 98.14% for natural and biochar prina, respectively.

Vithalkar and Jugade (2020) have carried out a study of CV removal with chitosan-coated bentonite. Similar to this study, in the adsorbent dosage versus removal efficiency experiments, they obtained a constantly increasing removal efficiency despite the increasing adsorbent dosage. Wang et al. (2020) carried out CV removal studies with activated sugarcane adsorbent. The adsorbent dosage versus removal efficiency study obtained 90% removal efficiency at the adsorbent dosage of 3.33 g/L and the removal efficiency remained constant at increasing adsorbent dosages.
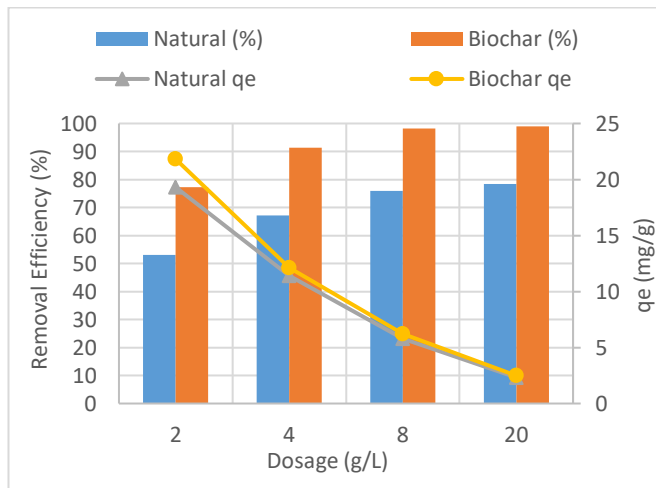
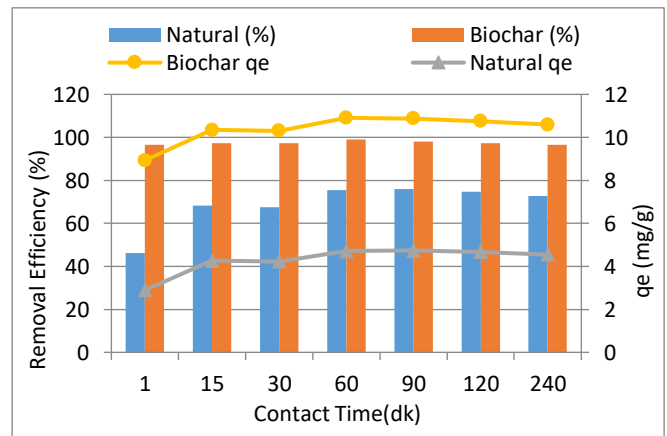**Fig. 1** Effect of dosage natural and biochar prina on removal efficiency

3.2 Effect of contact time on removal

To determine the effect of contact time on adsorption, experiments were conducted under general adsorption conditions for 1-15-30-60-90-120-240 minutes.

Figure 2 gives the results of removal efficiency and adsorption capacity. According to the results, biochar prina has much higher removal efficiency than natural prina. The biochar prina quickly reached equilibrium from the first minute and with rising contact times, removal efficiency was very low. The natural prina reached equilibrium after 60 minutes. Removal efficiencies obtained with natural and

biochar prina in 60 minutes selected as the optimum contact time were obtained as 75.44% and 99.10%, respectively.

Vithalkar and Jugade (2020) in their contact time study with chitosan-coated bentonite CV removal efficiency, reached the equilibrium time at 20 minutes. After this period, they obtained an almost constant removal efficiency. Priya et al. (2020) studied CV removal with active tropical fruit peels and commercial activated carbon. In their contact time study, they stated that the adsorption reached equilibrium within 30 minutes. Besides, they obtained the highest removal efficiency as 98% with commercial activated carbon adsorbent.

Fig. 2 Effect of contact time natural and biochar prina on removal efficiency

3.3 Effect of initial concentration on removal To determine the effect of the initial CV dye on adsorption, removal studies were carried out at the initial concentrations of 50-10-200-400-600-800 mg/L.

The results of concentration experiments are given in Figure 3. Biochar prina has high removal efficiency as well as other dosage and contact time studies. The removal efficiency was almost constant at lower initial concentrations, while a reduction was observed after 400 mg/L initial concentration. Therefore, an initial concentration of 50 mg/L was chosen for use in adsorption experiments. The highest removal efficiency was calculated as 75.85% and 98.14% for natural and biochar prina, respectively.
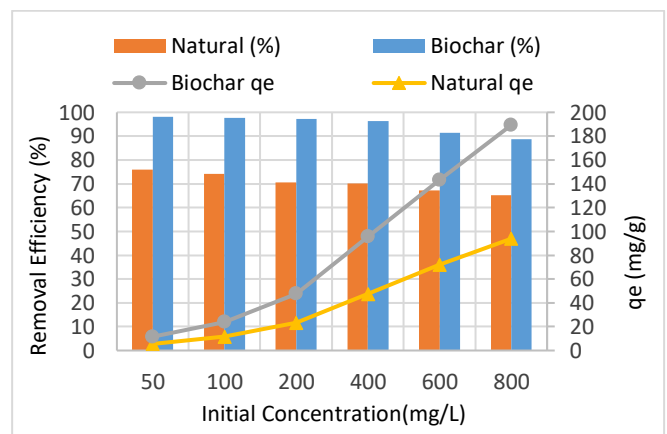
Fig. 3 Effect of initial concentration natural and biochar prina on removal efficiency

Wang et al. (2020), in their removal study with active sugarcane adsorbent against the initial CV concentration, achieved a partially decreasing removal efficiency with increasing initial concentration. They also stated that similar to this study, the adsorption capacity (q_e) increased rapidly from the 200 mg/L concentration to the 1000 mg/L concentration.

3.4 Adsorption isotherms

Initial concentration experimental data were applied to Langmuir and Freundlich isotherm models to determine the CV dye adsorption mechanism on natural and biochar prina.

The Langmuir equation is valid for single layer adsorption on the surfaces of a finite number of identical areas, and the Langmuir isotherm equation can be written as Equation 3;

$$\frac{C_e}{q_e} = \frac{1}{(q_m x K_L)} + \frac{C_e}{q_m} \qquad (3)$$

There, q_e, the amount adsorbed per unit weight of adsorbent (mg/g), C_e is the equilibrium concentration of adsorbate in solution after adsorption (mg/L), q_m and K_L are the Langmuir constants related to the saturated monolayer sorption capacity and the sorption equilibrium constant, respectively. (Rangabhashiyam et al. 2018).

The Freundlich isotherm is an empirical model that is based on adsorption on the heterogeneous surface area. The Freundlich equation is used to describe heterogeneous systems and is as in Equation 4 in logarithmic form.

$$\log q_e = \log K_F + \frac{1}{n x \log C_e} \qquad (4)$$

There, q_e is the amount of dye adsorbed per adsorbent of dye adsorbent (mg/g) is the equilibrium concentration in Ce (mg/L), K_F and n are empirical Freundlich constants, indicative of adsorption capacity and adsorption density, respectively (Dönmez and Aksu 2002).

Correlation coefficients with Langmuir and Freundlich parameters are given in Table 2. The suitability of adsorption to the isotherm model is expressed by the proximity of R^2 to 1. Accordingly, natural and biochar prina R^2 values were found to be suitable for the Freundlich model as 0.927 and 0.998, respectively.

Table 2 Correlation coefficients of isotherm models

Isotherm Model	Parameter	Natural Prina	Biochar Prina
Freundlich	k_F (L/g)	1.34	5.56
	n	0.75	1.27
	R^2	0.927	0.983
Langmuir	q_{max} (mg/g)	133.3	169.4
	K_L (L/mg)	0.010	0.028
	R^2	0.218	0.886

3.5 Adsorption kinetics

In order to research the adsorption mechanisms and potential rate-controlling step of CV removal, three standard kinetic models, such as the pseudo-first-order model (Lagergren 1898), pseudo-second-order model (Ho and McKay 1998) and intra-particle diffusion model (Tan et al. 2009). The correlation coefficients (R^2) were represented in Table 3.

Table 3 Parameters of adsorption kinetic models

Kinetic Models	Parameter	Natural Prina	Biochar Prina
Pseudo First Order	k_1 (min^{-1})	6.67×10^{-3}	4606×10^{-4}
	qe (mg/g)	2.07	6.30
	R^2	0.13	0.0018
Pseudo Second Order	k_2 (g/mg.dk)	11.58	0.29
	qe (mg/g)	4.59	6.04
	R^2	0.999	0.999
Intraparticle Diffusion	k_i (mg/g.min^2)	0.0985	0.0002
	C	3.53	6.09
	R^2	0.529	0.0003

Since the highest R^2 values are obtained in the pseudo-second-order kinetic model, adsorption is suitable for this model for both natural and biochar adsorbents. These results suggested that both physical and chemical adsorption might be involved in the adsorption process. Two consecutive stages could reason this phenomenon: the could be driven to access or into the pores of the adsorbent by the concentration gradient at the initial stage; after that, the CV ions did not diffuse into the pores of prina for further reactions until the surface functional sites were occupied fully. Based on this, CV's adsorption process in aqueous solution might only happen on the surface of prina and even the monolayer adsorption on the outer-sphere surface of complexes. To lend credence to this, focusing on the pseudo-second-order model.

4 Conclusion

Optimum adsorption conditions for CV removal with natural and biochar prina adsorbent were determined as 50 mg/L initial CV concentration, 8 g/L adsorbent dosage and 60 min contact time. The highest removal efficiencies obtained were 75.44% and 99.10% for natural and biochar prina, respectively. Likewise, the highest qe values were 93.86 mg/g and 95.43 mg/g for natural and biochar prina. These values are higher than in many studies in the literature. It has been observed that the adsorption mechanism fits the Freundlich isotherm model and pseudo-second-order kinetic model for both natural and biochar prina. The results obtained have shown that high-efficiency, cheap and abundant waste prina can be used as a suitable adsorbent in CV removal. Biochar prina has shown 20-50% higher removal efficiency than the natural form of prina. The high efficiency of dye removal is also of great importance in terms of turbidity. Therefore, thermal treatment is not an unnecessary step and the use of

biochar prina will provide much higher removal efficiencies. This study will contribute to such studies in the literature.

Authors' contributions: Sevda Esma Darama was interested in calculating the results, interpreting the data and arranging them according to the format. Özlem Uçar was interested in performing the experiments. Semra Coruh was interested in organizing the study.

Conflict of interest disclosure: Our work has not been carried out with any organization or employees.

References

Akar T, Tosun I, Ozkara Z, Yeni O, Sahin E, Akar S (2009) An attractive agro-industrial by-product in environmental cleanup: dye biosorption potential of untreated olive pomace. J Hazard Mater 166:1217-1225

Cheruiyot GK, Wanyonyi WC, Kiplimo JJ, Maina EN (2019) Adsorption of toxic crystal violet dye using coffee husks: equilibrium, kinetics and thermodynamics study. Scient African 5:e00116

Demiral I, Şamdan CA (2016) Preparation and characterisation of activated carbon from pumpkin seed shell using H_3PO_4. Anadolu Uni J Sci and Tech 17:125-138.

Dönmez G, Aksu Z (2002) Removal of chromium (VI) from saline wastewaters by Dunaliella species. Proc Biochem 38:751–762

Georgieva VG, Gonsalvesh L, Tavlieva M (2020) Thermodynamics and kinetics of the removal of nickel (II) ions from aqueous solutions by biochar adsorbent made from agro-waste walnut shells. J Mol Liq 312:112788.

Ho YS, McKay G (1998) Sorption of dye from aqueous solution by peat. Chem Eng J 70:115-124

Lagergren S (1898) Zur theorie der sogenannten adsorption geloester stoffe. Veternskapsakad Handlingar 24:1-39

Kaya N, Arslan F, Uzun ZY (2020) Production and characterization of carbon-based adsorbents from waste lignocellulosic biomass: their effectiveness in heavy metal removal. J Fuller, Nanot and Carbon Nanostr 28:769-780.

Malkoc E, Nuhoğlu Y, Dündar M (2006) Adsorption of chromium(VI) on pomace-an olive oil ındustry waste: batch and column studies. J Hazard Mater 138:142-151

Priya R, Stanly S, Dhanalekshmi SB, Mohammad F, Lohedanc HA (2020) Comparative studies of crystal violet dye removal between semiconductor nanoparticles and natural adsorbents. Optik 206:164281

Qiu Z, Chen J, Tanga J, Zhang Q (2018) A study of cadmiumremediation andmechanisms: Improvements in the stability of walnut shell-derived biochar. Sci of the Total Environ 636:80–84.

Rangabhashiyam S, Anu N, Selvaraju N (2013) Sequestration of dye from textile industry wastewater using agricultural waste products as adsorbents. J Environ Chem Eng 1:629-641

Rangabhashiyam S, Lata S, Balasubramanian P (2018) Biosorption characteristics of methylene blue and malachite green from simulated wastewater onto Carica papaya wood biosorbent. Surf and Interf 10:197–215

T.C. Ministry of Commerce (2019) Olive and olive oil report for 2018. Artisans, Artisans and Cooperatives General Directorate. https://ticaret.gov.tr/data/5d41e59913b87639ac9e02e8/3acedb62acea083bd15a9f1dfa551bcc.pdf of subordinate document. Accessed 16 October 2019

Tan IAW, Ahmad AV, Hameed BH (2009) Adsorption isotherms, kinetics, thermodynamics and desorption studies of 2,4,6-trichlorophenol on oil palm empty fruit bunch-based activated carbon. J. Hazard. Mater. 164:473–482

Toumi KH, Benguerba Y, Erto A, Dotto G, Khalfaoui M, Tiar C, Amrane A (2018) Molecular modeling of cationic dyes adsorption on agricultural Algerian olive cake waste. J Mol Liq 264:127-133

Vithalkar SH, Jugade RM (2020) Adsorptive removal of crystal violet from aqueous solution by cross-linked chitosan coated bentonite. Mater Today: Proc 29:1025-1032

Wang RF, Deng LG, Li K, Fan XJ, Li W, Lu HQ (2020) Fabrication and characterization of sugarcane bagasse–calcium carbonate composite for the efficient removal of crystal violet dye from wastewater. Ceramics Intern doi: 10.1016/j.ceramint.2020.07.237

Bulletin of Biotechnology

Computational study on pazopanib and pemetrexed anticancer drug molecules interacting with a small peptide link

Merve GÜREŞCİ*[iD], Güliz AK[2][iD], Habibe YILMAZ[2][iD], Şenay HAMARAT ŞANLIER[2][iD], Armağan KINAL[1][iD]

*[1]Ege University, Science Faculty Department of Chemistry, IZMIR, TURKEY
[2] Ege University Science Faculty Department of Biochemistry, IZMIR, TURKEY

Abstract: Cancer is a group of diseases that are defined as uncontrolled cell proliferation, impaired function of vital tissues, and cell death. Chemotherapy is a treatment using anti-cancer drugs to destroy cancer cells or control the growth of these cells. In chemotherapy applications pharmacologically active anticancer drugs reach with low specificity to tumor tissue, and their toxicity is dose dependent. Classical drug administration routes are either oral or intravenous. Orally taken pills result in irregular pharmacokinetics due to the passages of different metabolic pathways and their low specificity. This leads to frequent damage to healthy tissues. Nanoparticle-containing drug delivery systems may overcome these harmful side effects partially (or sometimes totally). Binding peptide-drug conjugates inside of some appropriate nanoparticles is one of the prominent methods among targeted drug delivery systems. Such a system containing Pazopanib (Pz) and Pemetrexed (Pm) drug complexes attached to magnetite nanoparticles with a short polypeptide chain (Ala-Lys-Ala-Leu-Arg-Cys) were designed in our laboratory. In the present study, we have computationally investigated the conjugation mechanisms of Pz and Pm drug molecules to the above-mentioned polypeptide chain. The stable structures on the complex formation pathways and their free energy values were obtained at the B3LYP/6-31G(d) level in the water. The mechanism of Pept-Pz complex formation has two steps whose free energy barriers are found to be 21.37 and 27.72 kcal/mol. On the other hand, the free energy barrier of the Pept-Pm complex having a single-step mechanism was calculated as 28.16 kcal/mol.

Keywords: Anticancer drugs; Pemetrexed; Pazopanib; DFT-B3LYP.

1 Introduction

Cancer is a critical and complex disease that occurs when the genes that control cell growth and division are damaged. The most important descriptive feature of cancer is abnormal cell divisions that occur in various parts of the body and can spread to other organs (Nayak and Pal 2010).

Today cancer is one of the diseases that pose a grave problem for all countries of the world. The International Cancer Research Organization (IARC) affiliated with the World Health Organization (WHO) for 2030 predicts that cancer will be in the first place among the causes of death (Tuncer 2008).

Cancer is a disease that takes a long time to develop. It provides convenience in the treatment of diagnosis in the early stages. If damaged cells can be intervened in the early stages of the mutation, cancer development can be stopped (Auyang 2006). Radiotherapy, chemotherapy, and surgery are the main methods used in cancer treatment. Surgical methods consist of resection (removal) of cancerous tissue.

The disadvantage of this method is the loss of an organ, risk of recurrence of cancer and inability to apply to all types of cancer (Thorn et al. 2017). In radiotherapy, the radiation distribution is not equal in density to all cancer cells, while in chemotherapy, cancer cells are killed by drugs that have toxic effects, causing healthy cells as well as cancer cells (Nehru and Singh 2008). The side effects that occur are caused by the fact that the methods in the treatments do not have a tissue-specific effect. Therefore, they became the most important medical problem in recent years.

Although there are many anti-cancer drugs on the market, it is realized that high toxicity and poor bioavailability pose the most important problem. At the same time, these drugs are not selective and affect both cancer cells and normal cells. Therefore, new, and selective and tumor-targeted drug delivery systems (Ak et al. 2019) need to be developed to combat such a lethal disease.

Advances in nanotechnology have brought important innovations in targeted drug delivery (Goel et al. 2009). In this way, while the intracellular concentrations of drugs in

cancer cells can be increased, their toxic effects on healthy cells can be minimized.

Today, it enables the diagnosis of diseases, determination of drug interactions, and delivery of coded packages with smart carrier systems to the relevant part of the body, especially due to its nanoparticular properties (Liu et al. 2008). As drug carriers, the reasons for using nanoparticles are as follows: their loading capacity is high, their surfaces can be modified by means of various molecules in order to reach the target more effectively due to not being recognized by the immune system. Since they cannot be recognized by the immune system, they can be designed to allow passage through physiological barriers such as blood-brain barrier and tight connections between cells.

Polymer-coated superparamagnetic materials can be used in diagnostic applications by allowing magnetic resonance visualization, and they have features such as enabling highly specific tissue targeting via conjugation with a ligand. (Soloviev 2007). The drug is directed to the target cell by ensuring that it is targeted to a specific area within the body with external stimuli (Vasir and Labhasetwar 2005). The magnetic targeting (Hamarat Şanlıer et al 2019) approach involves the injection of a therapeutic agent attached to or encapsulated into the carrier of the magnetic drug and orientation to the tumor tissue by externally applied localized magnetic field (Zhang et al. 2008). Magnetic targeting is a targeting method applied by using magnetic particles and magnetic field in order to concentrate the drugs in the targeted area and control the release of the drug (Widder and Senyei 1984). These drugs are generally toxic, non-durable, expensive and intended to be directed to a specific area for treatment. The magnetic field sensitive drug carriers contain materials such as magnetite, iron, nickel, and cobalt. Drug carriers can be magnetic liposomes, microspheres, nanospheres and colloidal iron oxide solutions.
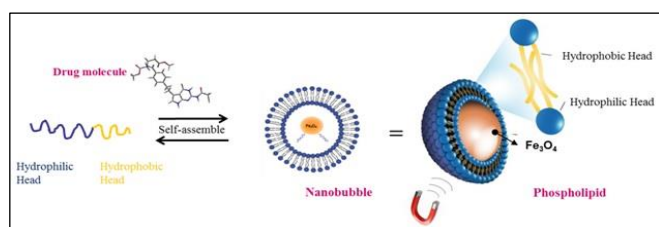


Fig. 1 Material formats of nanoparticle

Magnetic nanoparticle containing nano-conjugate is a hydrophilic material. The system called nano-bubble (Lin et al. 2014) consists of a short polypeptide chain and an anticancer drug complex bound to magnetite nanoparticles (Miklán et al. 2011). These nanoparticles are targeted by an external magnetic field. In addition, the binding of pharmaceutical carrier systems of different forms directly onto the biomolecule takes place via conjugation. Here, we present a computational study on conjugation mechanisms of anti-cancer Pemetrexed (Pm) and Pazopanib (Pz) drug molecules that are used in tumor targeted drug delivery systems to a short polypeptide chain (Ala-Lys-Ala-Leu-Arg-Cys).

2 Materials and Method

The most stable conformers of the peptide link, Pm, Pz, and their complexes were determined by the conformational analysis available in the Spartan'08 suite (Henre et al. 1986). The B3LYP method together with the 6-31G(d) basis set was employed for the determination of ground-state energies of the conformers. All the drug molecules, peptide and complexes as well as the transition state structures involved in the formation reaction mechanisms of the complexes have been optimized and characterized at B3LYP/6-31G(d) level of theory in water. The transition state structures connecting the reactants (intermediates) to the corresponding products were validated by the IRC (Internal Reaction Coordinate) calculations. The solvent effect was introduced with the Integral Equation Formalism Polarizable Continuum Model (IEFPCM, for water ε=80.6) (Tomasi et al. 1999). All calculations were performed with Gaussian 09 computational chemistry suite (Frisch et al. 2009).

3 Results and Discussion

The geometries of the polypeptide chain, Pm, and Pz molecules optimized at B3LYP/6-31G(d) level are shown in Figure 2. The polypeptide chain employed here is composed of Ala-Lys-Ala-Leu-Arg-Cys units. The chloro-acetylated forms of the drug molecules were utilized to be able to fuse with the polypeptide chain for the formation of the Pept-Pz and Pept-Pm complexes, respectively.
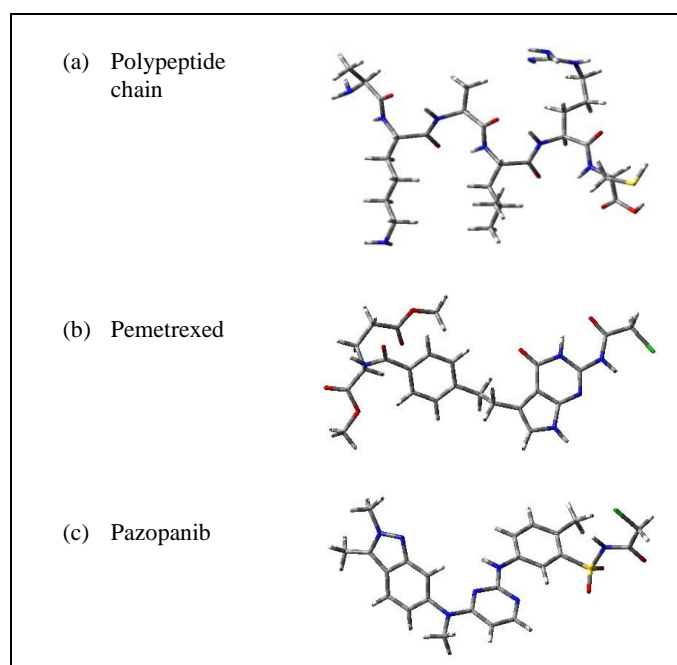
Fig. 2 Optimized geometries of (a) polypeptide chain, (b) Pm, and (c) Pz molecules calculated at the B3LYP/6-31G(d) level.

Figure 3 depicts the optimized geometries and frontier orbitals of the Pm, and Pz molecules calculated at the B3LYP/6-31G(d) level. In the PM molecule, both HOMO and LUMO are on the pyrrolo pyrimidine ring and chloroacetate. Similarly, the HOMO and LUMO of the Pz molecule are located on the dimethyl indazole and the adjacent pyrimidine ring. Consequently, the electron

densities of both drugs are mainly found to be concentrated on the fused five- and six-member ring moieties.
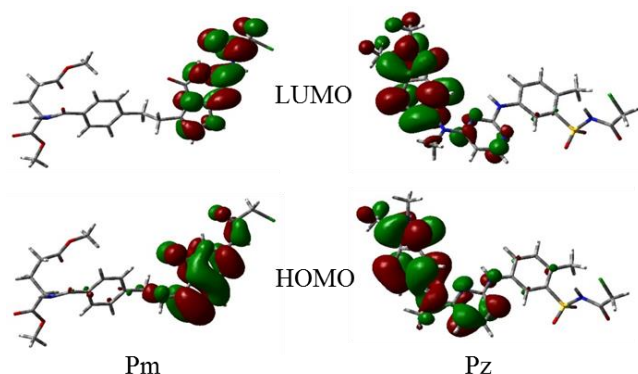
Fig. 3 Optimized geometries and frontier orbitals of the Pm and Pz molecules obtained at the B3LYP/6-31G(d) level.

Figure 4 shows the B3LYP optimized geometries of the Pept-Pz and Pept-Pz complexes. There are no significant conformational changes between the geometries of the free Pm and free Pz molecule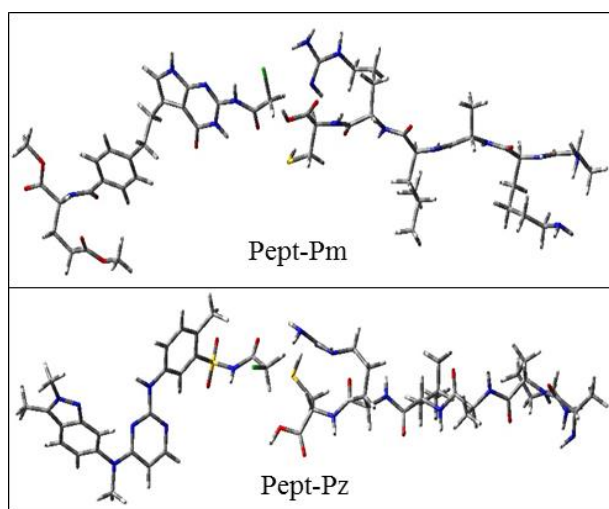s in water media and their geometries combined with the peptide. Conversely, the peptide molecule has subjected to a significant conformational change after combining with the drug molecules. This change stands out as elongation. Namely, the peptide molecule elongates when it is fused with the drug while it is compact when it is alone.

Fig. 4 Optimized geometries of Pept-Pm and Pept-Pz complex obtained at the B3LYP/6-31G(d) level.
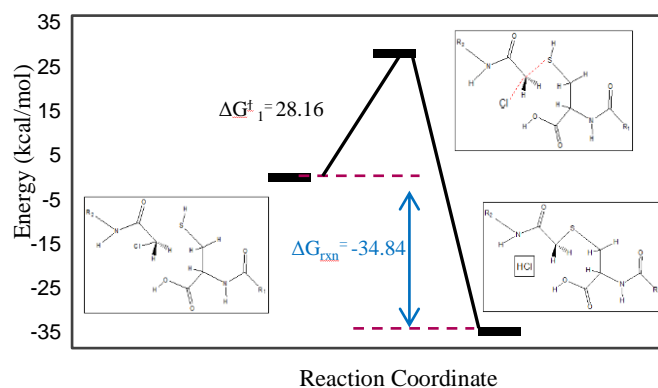
Fig. 5 The mechanism of Pept-Pm complex obtained at the B3LYP/6-31G(d) level in water.
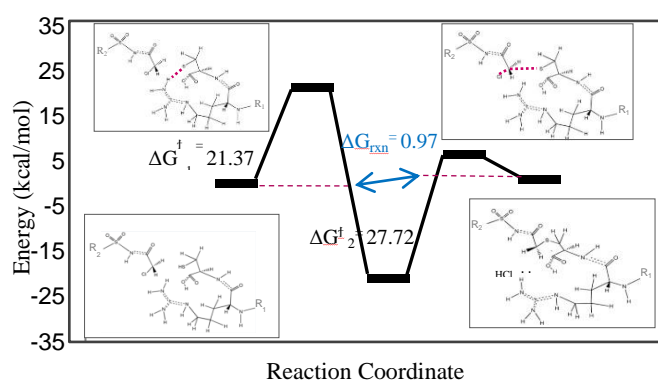
Fig. 6 The mechanism of Pept-Pz complex obtained at the B3LYP/6-31G(d) level in water.

The formation of the Pept-Pm complex has an exothermic single-step mechanism. The activation free energy barrier and the reaction free energy were calculated as 28.16 kcal/mol and -34.84 kcal/mol, respectively (Fig. 5). On the other hand, the formation of Pept-Pz complex occurs via a two-step exothermic mechanism as shown in Figure 6. As seen from the figure, the second step is the rate-determining step of the reaction. The activation free energy barrier and the reaction free energy were calculated as 27.72 kcal/mol and 0.97 kcal/mol, respectively. Table 1 gives activation and reaction enthalpies of the Pept-Pm complex.

Table 1 The activation and reaction enthalpies of the Pept-Pm and Pept-Pz complex obtained at B3LYP/6-31G(d) level

Complex	$\Delta H^{\ddagger}_{298}$ (kcal/mol)	ΔH^{rxn}_{298} (kcal/mol)
Pept-Pm	25.57	-38.11
Pept-Pz	23.58	-1.87

Pept-Pm and Pept-Pz complexes are formed by conjugation reaction of the chloro-acetylated Pm and Pz molecules with the peptide link. The possible reaction mechanism for the formation of both complexes is the sulfur-carbon bond formation mechanism (R'-S-CH2-R'') where the thiol group (–SH) of the cysteine amino acid in the peptide attacks the carbon of the chloroacetyl group of the drug.

4 Conclusion

In this study, the conjugation mechanisms of Pm and Pz drug molecules to the specified polypeptide chain (Ala-Lys-Ala-Leu-Arg-Cys) in an aqueous medium have been studied using the DFT-B3LYP method.

• Pept-Pz and Pept-Pm complexes are formed via the reactions between chloro-acetylated forms of the Pz, and Pm drug molecules and a specifically designed peptide link.

• The stable structures on the complex formation pathways and their free energies values were obtained at the B3LYP/6-31G(d) level.

• The free energy barrier of the Pept-Pm complex having a single-step mechanism was calculated as 28.16 kcal/mol.

• The mechanism of Pept-Pz complex formation has two steps whose free energy barriers were calculated as 21.37 and 27.72 kcal/mol. The second step is found to be the rate-determining step of the reaction.

Authors' contributions: The experimental part of the study was performed by Şenay HŞ, GA, HY, while the computational part was completed by AK and MG.

References

Ak G, Aksu D, Çapkın E, Sarı Ö, Kımız Gebelioğlu I, Hamarat Şanlıer Ş (2019) Delivery of pemetrexed by magnetic nanoparticles: design, characterization, in vitro and in vivo assessment. Preparative Biochemistry & Biotechnology 50:3, 215-225

Auyang YS (2006) Cancer Causes and Cancer Research on Many Levels of Complexity. Available at: http://www.creatingtechnology.org/biomed/cancer Accessed 20 Apr 2015

Frisch MJ, Trucks GW, Schlegel HB, Scuseria GE, Robb MA, Cheeseman JR et al. (2009) Gaussian 09, Revision D.01.Wallingford CT: Gaussian, Inc.

Goel HC, Kumar B, Yadav PR, Moshahid M, Rizvi A (2009) Recent developments in cancer therapy by use of nanotechnology. Digest J Nanomater Biostr 4(1):1-12

Hamarat Şanlıer Ş, Ak G, Yılmaz H, Ünal A, Bozkaya ÜF, Tanıyan G, Yıldırım Y, Türkyılmaz GY (2019) Development of Ultrasound-Triggered and Magnetic-Targeted Nanobubble System for Dual-Drug Delivery. Journal of Pharmaceutical Sciences 108-3 1272-1283

Hehre WJ, Radom L, Schleyer PVR, Pople JA (1986) Ab Initio Molecular Orbital Theory. John Wiley & Sons, Inc. USA 11-88

Lin CY, Javadi M, Belnap DM, Barrow JR, Pitt WG (2014) Ultrasound sensitive Liposomes containing doxorubicin for drug targeting therapy. Nanomedicine: Nanotechnology, Biology, and Medicine 10(1):67-76

Liu HL, Wu JH, Min JH, Kim YK (2008) Synthesis of monosized magnetic-optical AuFe alloy nanoparticles. Journal of Applied Physics Part 103(7):1-3

Miklán Z, Orbán E, Bánóczi Z, Hudecz F (2011) New pemetrexed-peptide conjugates: synthesis, characterization and in vitro cytostatic effect on non-small cell lung carcinoma (NCI-H358) and human leukemia (HL-60) cells. J Pept Sci 17(12):805-811

Nayak KA, Pal D (2010) Nanotechnology for targeted delivery in cancer therapeutics. Seeman-ta Institute of Pharmaceutical Sciences 1:1

Nehru MR, Singh PO (2008) Nanotechnology and cancer treatment. Asian J Exp Sci 22-2:45-50

Soloviev M (2007) Nanobiotechnology today: focus on nanoparticles. Journal of Nanobiotechnology 5(11):1-3

Thorn CF, Sharma MR, Altman RB, KleinTE (2017) PharmGKB summary: pazopanib pathway, pharmacokinetics. Pharmacogenet Genomics. 27(8): 307–312

Tomasi, J, Mennucci B, Cances E (1999) The IEF version of the PCM solvation method: an overview of a new method addressed to study molecular solutes at the QM Ab initio level. J. Mol. Struct, Theochem 464:211–226

Tuncer M (2008) Globalleşen Kanser ve Türkiye. Available at: www.nukte.org Accessed: 15 Mar 2015

Vasir JK, Labhasetwar V (2005) Targeted drug delivery in cancer therapy. Technology in Cancer Research and Treatment 4(4):363-374

Zhang L, Gu FX, Chan JM, Wang AZ, Langer RS, Farokhzad OC (2008) Nanoparticles in medicine: Therapeutic applications and developments. Clinical Pharmacology and Therapeutics 83:761-769

Widder KJ, Senyei AE (1984)'Magnetic albumin microspheres in drug delivery' Microsheres and Drug Therapy. Eda.: S.S. Davis, L.Illum, J.G.McVie, E. Tomlinson, Elsevier, Amsterdam 393-411

Bulletin of Biotechnology

The decolorization of synthetic dyes with immobilized *Bacillus* species

Elif Canpolat[1] , Tuba Artan Onat[2*] , Özge Çetin[2]

[1] *Faculty of Agricultural Sciences and Technologies, Nigde Omer Halisdemir University, Turkey*
[*2] *Department of Biotechnology, Nigde Omer Halisdemir University, Turkey*

Abstract: Although, synthetic dyes have toxic effects on to environment, are very important for coloration of large number of materials and lead to increasing concerns about color removal worldwide. Immobilization of microorganisms is one of the promising techniques for biological treatment of wastewater with the many advantages for industrial usage. This study aimed to determine the efficiency of immobilized four different *Bacillus* species (*B. cereus, B. megaterium, B. subtilis* and *B. thuringiensis*) on decolorization of dyes (maxilon red, methyl red and doracryl blue) at different Na-alginate concentrations. *B. megaterium* and *B. thuringiensis* were most effective and decolorized the maxilon red 92.63% and 90.74%, respectively, with the Na-alginate concentration of 2.5%. *B. megaterium* was the most effective strain in decolorization of doracryl blue with 75.91% decolorization value and with beads at 10% Na-alginate concentration. *B. megaterium* was the most effective strain in decolorization of methyl red with 64.99% decolorization and the beads were prepared with 10% Na-alginate concentration. Among the four *Bacillus* species *B. megaterium* was the most effective in the decolorization experiments of all three dyes. Results of this study could be used as a reference for the development of effective removal technique for dyes in textile wastewater.

Keywords: *Bacillus* species; Decolorization, Immobilization, Na-alginate, Methyl red, Maxilon red, Doracryl blue

1 Introduction

Synthetic dyes are frequently used in the cosmetics, textile, food, leather, papermaking and pharmaceutical industries due to their high stability, low cost and variety in color (Przystaś et al. 2018). Dyes are categorized in three groups as anionic, cationic and non-ionic dyes. Azo, anthraquinone and phthalocyanine groups of reactive dyes, which are hard to remove under aerobic conditions, are widely used in textile industry. The textile wastewater contains these dyes as pollutant in high concentrations. Removal of azo dyes from aqueous effluents is difficult, as they might be stable when they exposed to light and heat (Saravanan et el. 2013, Al-Fawwaz et al. 2016, Hameed and Ismail 2018, Nath et al. 2019).

In last two decades, the application of immobilization techniques attracted attention for decolorization of wastewater. In a variety of scientific and industrial applications of immobilized microbial enzymes, organelles, and cells have been widely used due to the economic view that could be useful application in research for industry. The immobilization technology is an ecofriendly technique, in which high removal yields can be achieved, compared to

physical and chemical processes or procedure that use not immobilized biological materials and reduces the secondary pollutants (Cassidy et al. 1996, Suganya and Revath 2006, Wen et al. 2018).

A wide variety of organisms, including bacteria, fungi, yeast, algae and plants, are capable of decolorizing dyes. The major problem in dye removal is the toxic effect of dyes on microorganisms. Therefore, a good method to increase the concentration of microorganisms and to protect from toxicity is immobilization. The immobilized microorganisms are cost effective by using several times without significant loss of activity (Saratale et al. 2011).

Among the various developed methods for cell immobilizing the encapsulation in calcium alginate beads was used in this study. The Na-alginate that used for immobilization of microorganisms is easy to use, non-toxic to humans and the environment, are legally safe for human use, present in large quantities and an economic option. The major advantage of alginate is that it is not exposed to major changes in the physicochemical state during immobilization and that the gel is transparent and permeable (de-Bashan and Bashan 2010).

This study aimed to decolorize of synthetic dyes (maxilon red, methyl red and doracryl blue) present in industrial wastewaters with different *Bacillus* species (*Bacillus cereus*, *Bacillus megaterium, Bacillus subtilis* and *Bacillus thuringiensis*) by immobilization method with Na-alginate. The effect of Na-alginate concentrations were also determined on decolorization ratio.

2 Materials and Method

2.1 The synthetic dyes

The synthetic dyes MR, the MeR, The DB (is a basic dye) were used in this study and obtained from textile industry in Niğde (Birko Carpet Factory) and Figure 1 shows the chemical structure of the dyes (El-Syed et al. 2014, Vatandoostarani et al. 2017). The stock solution of the dye was prepared by membrane filtration at 10000 mg/L concentration. The maximum absorbans (λmax) of the each dye was determined at 430 nm for MeR, at 515 nm for MR and at 600 nm for DB by UV-Visible spectrophotometer (Jenway).
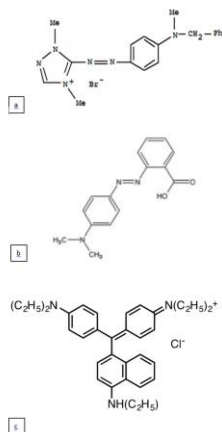

Figure 1. The chemical structure of synthetic dyes a) MR (El-Syed et al. 2014) b) the MeR (Vatandoostarani et al. 2017). c) The DB (is a basic dye)

2.2 Growth conditions for *Bacillus* species

The bacterial strains used in this study, *Bacillus thuringiensis*, *Bacillus cereus*, *Bacillus subtilis*, *Bacillus megaterium* were obtained from Niğde Ömer Halisdemir University, Biotechnology Department, Turkey. The bacterial cultures were grown in nutrient agar medium containing 5g peptone, 5g NaCl, 3g beef extract in 1L and incubated for 48h at 30°C under static conditions for sporulation. The medium was autoclaved at 121 °C for 15 min and the *Bacillus* species were grown at sterile conditions. The sporulated pure cultures of *Bacillus* species were used for immobilized beads (Amin et al. 2015).

2.3 Preparing of immobilized beads

In this study, four different concentrations of Na-alginate (1%, 2.5%, 5%, and 10%) were tested to determine the optimum Na-alginate concentration. Bacterial cultures were

collected from petri dishes as 0.5 g sporulated bacteria and washed with 0.85% NaCl solution. The washed bacterial cultures were used for making Na-alginate beads and were mixed with different concentration Na-alginate solutions. The prepared solutions of bacteria and Na-alginate was dripped in 0.1 M CaCl$_2$.2H$_2$O solution with a syringe to obtain the immobilized beads (Fig.2). By replacement of sodium and calcium ions, bacterial cells were trapped in alginate gel. After 30 minutes for hardening, the beads were filtered out and stored in 0.05 M CaCl$_2$.2H$_2$O in the refrigerator for further studies. Beads did not prepared at sterile conditions and were washed with 0,85 % NaCl before experimental steps (Moreira Santos et al. 2002, Ogugbue et al. 2012).

Figure 2. The preparation of immobilized beads

2.4 Decolorization experiments

Decolorization studies were conducted in batch conditions at room temperature and the immobilized cells of *Bacillus* species were prepared with four different Na-alginate concentrations. Bio-beads of *Bacillus* species were made with 1%, 2.5%, 5%, 10% Na-alginate concentrations and 10 gram bio-beads transferred into 250 mL ErlenMeyer flasks which were containing 100 mL dye solution at 100 mg/L initial dye concentration. The flasks were kept at room temperature and the samples were taken in every 24 hours for ten days. The maximum absorbance was measured by spectrophotometer (Jenway). The dye decolorization yield was calculated with given formula below (Eq. 1). The C0 indicates that the dye concentration at the beginning and the Cf indicates that the dye concentration at the end of decolorization period (Castro et al. 2017).

$$\text{Decolorization Yield\%} = \frac{Co - Cf}{Co} * 100 \text{ (Eq. 1)}$$

3 Results and Discussion

Bioremediation is usage of microorganisms such as bacteria, fungi or algae to reduce, eliminate or treat the pollutants present in soils, sediments, water, and air The dye decolorization capacity of different types of microorganisms is affected by several conditions such as nutrients, pH, temperature and initial dye concentration. (Gül and Dönmez 2013, Gül 2018). The influence of immobilization technique

with different type of microbial cells were reported and worked elsewhere before. Immobilized cells is used for wastewater treatment and color removal because of facilitates the separation and recovery of the immobilized bacteria and binding agent, and makes it usable by reducing the total cost also (Ha et al. 2009, Hyde et al. 1991, Zeroual et al. 2001). Therefore, this work focused only on the immobilization technique and the effect of Na-alginate concentration on dye decolorization. This work is about the dye decolorization capacity of different *Bacillus sp.*, the dye concentrations and decolorization yield of immobilized cells. The results were shown with following graphics for synthetic dyes and *Bacillus* species separately (Figures 3a,b,c,d, 4a,b,c,d, 5a,b,c,d).

3.1 The Maxilon red decolorization

The beads that prepared with 2.5% Na-alginate concentration and *B. megaterium* were demonstrated the highest removal yield, which was 92.63% at ten days decolorization period. The other *B. megaterium* beads, which were prepared with 1%, 5% and 10% Na-alginate concentrations the dye removals were, determined as 55.99%, 60.72% and 48.94% respectively (Fig.3d).

The *B. thuringiensis* beads demonstrated similar dye removal capacity to the *B. megaterium* with 2.5% Na-alginate beads as 90.74% decolorization. The MR decolorization was determined as 50.75%, 44.74%, and 43.44% for 1%, 5% and 10% Na-alginate sequentially for beads of *B. thuringisensis* (Fig. 3a).
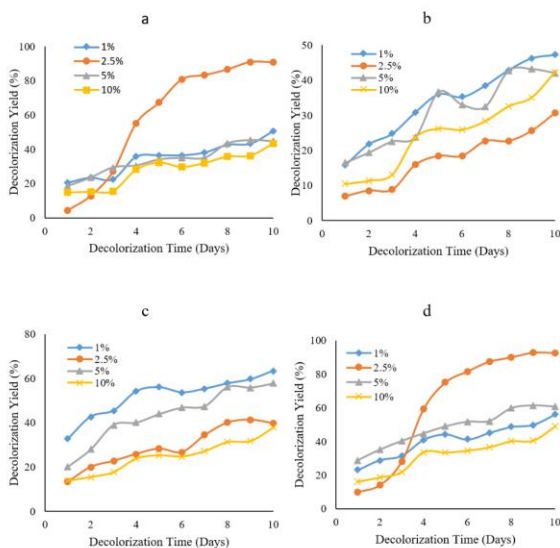

Figure 3. The MR decolorization with *Bacillus* species a) *B. thuringiensis* b) *B. cereus* c) *B. subtilis* d) *B. megaterium*
Blue, orange, grey and yellow lines refer to 1%, 2.5%, 5%, 10% Na-alginate concentration sequentially

B. subtilis was showed at 63,49% ratio that the maximum decolorization with 1% Na-alginate concentration at decolorization period. The beads which were prepared with 5% Na-alginate concentration showed 57.75% removal of MR and the 2.5% and 10% Na-alginate concentration

demonstrated at 39.74% and 37.90% dye removal sequentially (Fig. 3c).

The lowest degrees of dye decolorization for MR were determined with the *B. cereus* beads and the maximum MR decolorization with *B. cereus* was determined as 47.25%. The 5% and 10% Na-alginate beads with *B. cereus* were showed 42% decolorization both and the lowest dye decolorization ratio for MR was determined for 2.5% Na-alginate-*B.cereus* beads as 30% removal (Fig. 3b).

The maxilon red decolorization was tested with immobilized *Phanerochaete chrysosporium* (1557) mycelium with kissiris that decolorized at maximum ratio (Karimi et al. 2009). Also electrooxidation and electrocoagulation technique could be used for MR decolorization (El-Sayed et al. 2014). In this work the maximum decolorization ratio was tested as 90% with immobilized *B. thuringisensis* with 2.5% Na-alginate concentration and this results are similar to other decolorization techniques for MR.

3.2. The doracryl blue decolorization

The doracryl blue was decolorized by only the 10% Na-alginate beads for all *Bacillus* species. The decolorization values, which showed at Figure 4, were determined as 10.49%, 26.49%, 25.16% and 75.91% for *B. thuringiensis* (Fig 4a), *B. cereus* (Fig. 4b), *B. subtilis* (Fig. 4c) and *B. megaterium* (Fig. 4d) respectively. The *B. megaterium* beads were the most effective biosorbents for DB. The other beads, which were prepared with 1%, 2.5% and 5% Na-alginate concentrations with all *Bacillus* species, showed approximately 5% dye decolorization.
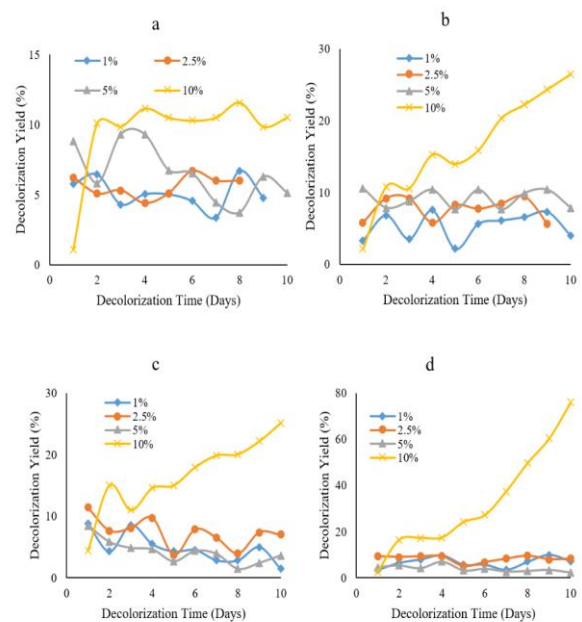

Figure 4. The DB decolorization with *Bacillus* species a) *B. thuringiensis* b) *B. cereus* c) *B. subtilis* d) *B. megaterium*
Blue, orange, grey and yellow lines refer to 1%, 2.5%, 5%, 10% Na-alginate concentration sequentially

Decolorization ratio of methylene blue with immobilized *B. subtilis* was determined as 80% and highest removal capacity of immobilized *Desmodesmus* sp. were determined for 5 mg/L initial methylene blue concentration. Moreover, *B. megaterium* was showed 90% Reactive Blue decolorization yield (Upendar et al. 2016, Erdem et al. 2019). In this work the immobilization of different *Bacillus* species were showed higher removal efficiency for DB at 10% Na-alginate concentration.

3.3 The methyl red decolorization

The decolorization of MeR by *B. megaterium* beads were more effective than the other *Bacillus* species. The 5% and 10% Na-alginate concentration were demonstrated 64,59% and 64,99% dye removal degree at decolorization period and the decolorization ratio of 1% and 2.5% Na-alginate concentrations were determined as 50.86% and 41.37% (Fig 5d).

The *B. subtilis* decolorized MeR at 40% approximately at 1%, 2.5% and 5% Na-alginate concentration. However, the beads that were prepared with 10% Na-alginate and *B. subtilis* and *B. cereus* removed the 54,84% and 54.23% of MeR from the decolorization solution (Fig. 5c).
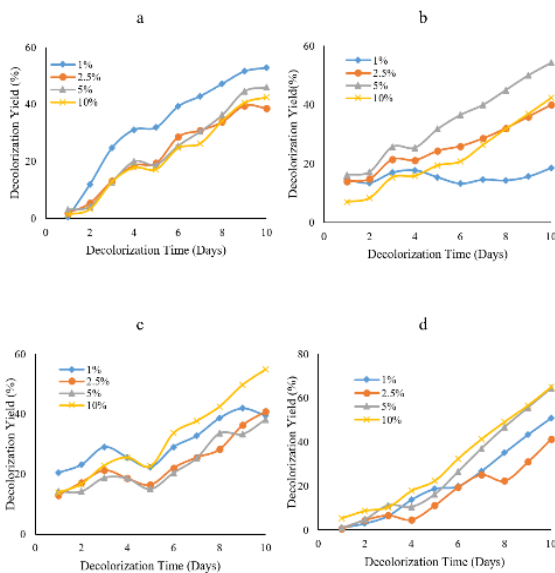

Figure 5. The MeR decolorization with *Bacillus* species a) *B. thuringiensis* b) *B. cereus* c) *B. subtilis* d) *B. megaterium* Blue, orange, grey and yellow lines refer to 1%, 2.5%, 5%, 10% Na-alginate concentration sequentially

The *B. thuringiensis* and 1% Na-alginate beads demonstrated similar dye removal capacity to the *B. subtilis* and *B. cereus* beads as 52.80% decolorization. The MeR decolorization was determined as 38.56%, 45.92%, 42.46% for 2.5%, 5% and 10% Na-alginate concentration sequentially for beads of *B. thuringisensis* (Fig. 5a,b,c).

Extensive studies have been performed to determine the role of the diverse groups of bacteria in the decolorization of different textile dyes. Similar to that of free cells, studies were

also carried out using immobilized beads. A similar study was observed with the Reactive Yellow 17 and Reactive Blue 36 dyes of immobilized *B. licheniformis* strain. Cells immobilized with sodium alginate showed maximum color removal compared to free cells (Suganya and Revath 2006). In a study in which methylene blue, which is widely used in cotton and silk, was selected as a model dye, the biological removal of MB using *Bacillus subtilis* immobilized with Ca-alginate was tested in both batch and continuous contactors. More than 90% removal has been achieved during kinetic study in batch contactor (Upendar et al. 2016). Decolorization of the Maxilon red dye by *Phanerochaete chrysosporium* fungus immobilized in the trickle-bed reactor (TBR) using basal nitrogen-limited growth medium showed a color removal of approximately 94% in 4-5 days (Karimi et al. 2009).

Table 1. The summarized decolorization yields of *Bacillus* species

	MR		DB		MeR	
	Na-alg. conc. (%)	Decol. Yield (%)	Na-alg. conc. (%)	Decol. Yield (%)	Na-alg. conc. (%)	Decol. Yield (%)
B. thuringiensis	2.5	90.74	10	10.49	1	52.8
B. cereus	1	47.25	10	26.49	5	54.23
B:subtilis	1	63.49	10	25.16	10	54.84
B. megaterium	2.5	92.63	10	75.91	10	64.99

The results mentioned above in this work summarized in the Table 1, that were showed *B. thuringiensis*, and *B. megaterium* beads, which were prepared with 2.5% Na-alginate concentration, could be able to remove almost 90% of dye at decolorization solution. The Na-alginate-*Bacillus* beads were not effective to remove the DB, only 10% Na-alginate beads were decolorized the DB at ten days decolorization period. In addition, the MeR decolorization was approximately 50% with all *Bacillus* species. Besides, not only the 10% Na-alginate - *B. megaterium* beads were showed the maximum dye decolorization effect on the DB with 75% and MeR with 65% but also the 2.5% Na-alginate - *B. megaterium* beads removed the 92% of MR at the same decolorization period.

Bacillus sp. are effective microorganisms for removal of different dyes or textile effluent. Although, different microorganisms are useful for dye decolorization such as *Corynebacterium sp.* or *Pseudomonas sp.* (Gül 2018). *Bacillus sp.* was used for removal of Acid Red 2, Acid Orange 7, Remazol Black B and Congo Red and the removal rate were found as 90-100% (Jaiswal and Gomashe 2017, Shah et al. 2013). However, the *Bacillus subtilis* was removed the textile effluent at 63% decolorization rate (Sivaraj et al. 2011).

Bacterial decolorization is inexpensive and ecofriendly method and immobilization is very efficient method. In general, immobilized cells are more tolerant to factors such as temperature, pH and the presence of inhibitory compounds.

Na-alginate is non-toxic and suitable for use in gelation, so that immobilization with Na-alginate is an acceptable matrix material and is satisfactory for use with microorganisms (Sriamornsak and Nunthanid 1998, Tallur et al. 2009). The results showed that the decolorization of synthetic dyes and immobilized *Bacillus* species cells would be used for decolorization of different dyes at textile wastewater. The *Bacillus* species could be used for biodegradation as immobilized cells promisingly.

4 Conclusion

Many researchers have studied the environmental effects of synthetic dyes and their removal and this study aimed to determine the dye decolorization capacity of the immobilized *Bacillus* sp. It was understand from the results above mentioned that the *B. megaterium* was more effective than the other *Bacillus* species that were used ın the study. The *B. subtilis, B. cereus* and *B. thuringiensis* beads were affect by Na-Alginate concentrations and higher Na-alginate concentrations reduced the dye decolorization ratio. However the bio-beads that were made with *B. megaterium* and 10% Na-alginate concentration showed higher decolorization yields and they were decolorized the MR at 92%, DB at 75% and MeR at 65% at ten day decolorization period. In the light of these results, *B. megaterium* should be use for MR, MeR or DB decolorization as immobilized beads.

Acknowledgements

Authors' contributions: Elif CANPOLAT worked on the process of conducting and maintaining the experiments and writing the article. Dr. Tuba ARTAN ONAT worked on the writing and sending and follow-up of the article. Özge ÇETİN worked during the experiments.

References

Al-Fawwaz AT, Abdullah M (2016) Decolorization of Methylene Blue and Malachite Green by Immobilized *Desmodesmus* sp. Isolated from North Jordan, Int J Environ Sci Dev 7(2):95-99

Amin M, Rakhisi Z, Ahmady AZ (2015) Isolation and Identification of *Bacillus* Species From Soil and Evaluation of Their Antibacterial Properties. Avicenna J Clin Microb Infec 2(1):1-4

Cassidy MB, Lee H, Trevors JT (1996) Environmental applications of immobilized microbial cells: a review. J Ind Microbiol 16:79-101

Castro KC, Cossolin AS, Reis HCO, Morais EB (2017) Biosorption of anionic textile dyes from aqueous solution by yeast slurry from brewery. Braz Arch Biol Technol 60:1-13

De-Bashan LE, Bashan Y (2010) Immobilized microalgae for removing pollutants: review of practical aspects. Bioresour Technol 101(6):1611-1627

El-Sayed GO, Awad MS, Ayad ZA (2014) Electrochemical Decolorization of Maxilon Red GRL Textile Dye. Int Res J Pure Appl Chem 4(4):402-416

Erdem, Ö, Erkan Türkmen K, Aracagök D, Cihangir N (2019) Decolorization of Reactive Blue 19 Dye by *Bacillus megaterium* Isolated From Soil. Hacettepe J Biol Chem 47(2):193-201

Ha J, Engler CR, Wild JR (2009) Biodegradation of coumaphos, chlorferon and diethylthiophosphate using bacteria immobilized in Ca-alginate gel beads. Biores Technol 100(3):1138-1142

Hameed B, Ismail Z (2018) Decolorization, biodegradation and detoxification of reactive red azo dye using non-adapted immobilized mixed cells. Biochem Eng J 137:71–77

Hyde FW, Hunt GR, Errede LA (1991) Immobilization of bacteria and *Saccharomyces cerevisiae* in poly (tetrafluoroethylene) membranes. Appl Environ Microbiol 57(1):219–222

Gül ÜD, Dönmez G (2013) Application of mixed fungal biomass for effective reactive dye removal from textile effluents. Desalin Water Treat 51 (16-18):3597-3603

Gül ÜD (2018) Bioremediation of Dyes in Textile Wastewater. Turkish J Sci Rev 11(2): 24-28

Jaiswal SS, Gomashe AV (2017) Bioremediation of textile azo dyes by newly isolated *Bacillus* sp. from dye contaminated soil. Int J Biotechn Biochem 13 (2):147-153

Karimi A, Vahabzadeh F, Mohseni M, Mehranian M (2009) Decolorization of Maxilon-Red by Kissiris Immobilized *Phanerochaete chrysosporium* in a Trickle-Bed Bioreactor-Involvement of Ligninolytic Enzymes. Iran J Chem Chem Eng 28(2):1-13

Moreira dos Santos M, Moreno-Garrido I, Goncalves F, Soares AMVM, Ribeiro R (2002) An in situ bioassay with microalgae for estuarine environments. Environ Toxicol Chem 21(3):567–574

Nath J, Bag S, Bera D, Ray L (2019) Biotreatment of malachite green from aqueous solution and simulated textile effluent by growing cells (batch mode) and activated sludge system. Groundw Sustain Dev 8:172-178

Ogugbue CS, Morad N, Sawidis T, Oranusi NA (2012) Decolorization and partial mineralization of a polyazo dye by *Bacillus firmus* immobilized within tubular polymeric gel Biotech 2(1):67–78

Przystaś W, Zabłocka-Godlewska E, Grabińska Sota E (2018) Efficiency of decolorization of different dyes using fungal biomass immobilized on different solid supports. Environ Microbiol 49(2):285-295

Saratale RG, Saratale GD, Chang JS, Govindwar SP (2011) Bacterial decolorization and degradation of azo dyes: A review. J Taiwan Inst Chem E 42(1):138–157

Saravanan N, Kannadasan TC, Basha A, Manivasagan V (2013) Biosorption of Textile Dye Using Immobilized Bacterial (*Pseudomonas aeruginosa*) and Fungal (*Phanerochate chrysosporium*) Cells. Am J of Environ Sci 9(4):377-387

Shah MP, Patel KA, Nair SS, Darji AM (2013) An Innovative Approach to Biodegradation of Textile Dye (Remazol Black B) by *Bacillus* Spp. Int J Environ Bioremediat Biodegradat 1 (2):43-48

Sivaraj R, Dorthy CAM, Venckatesh R (2011) Isolation, Characterization and growth Kinetics of Bacteria metabolizing Textile Effluent. J Biosci Tech 2(4):324-330

Sriamornsak P, Nunthanid J (1998) Calcium pectinate gel beads for controlled release drug delivery: I. Preparation and in vitro release studies. Int J Pharm 160(2):207-212

Suganya K, Revath K (2006) Decolorization of Reactive Dyes by Immobilized Bacterial Cells from Textile Effluents. Int J Curr Microbiol and Appl Sci 5(1):528-532

Tallur PN, Megadi VB, Ninnekar HZ (2009) Biodegradation of p-cresol by immobilized cells of *Bacillus* sp. strain PHN 1. Biodegradation 20(1):79–83

Upendar G, Duttaa S, Chakrabortyb J, Bhattacharyyac P (2016) Removal of methylene blue dye using immobilized *Bacillus subtilis* in batch & column reactor. Materials Today: Proceedings 3(10):3467–3472

Vatandoostarani S, Lotfabad TB, Heidarinasab A, Yaghmaei S (2017) Degradation of azo dye methyl red by *Saccharomyces cerevisiae* ATCC 9763. Int Biodeterior Biodegradation 125:62-72

Wen X, Du C, Zeng G, Huang D, Zhang J, Yin L, Tan S, Huang L, Chen H, Yu G, Hu X, Lai C, Xu P, Wan J (2018) A novel biosorbent prepared by immobilized *Bacillus licheniformis* for lead removal from wastewater. Chemosphere 200:173-179

Zeroual Y, Moutaouakkil A, Blaghen M (2001) Volatilization of mercury by immobilized bacteria (*Klebsiella pneumoniae*) in different support by using fluidized bed bioreactor. Curr Microbiol 43(5):322–327

Bulletin of Biotechnology

Bioactivities of extracts and isolated compounds of *Vachellia leucophloea* (Roxb.) Maslin, Seigler & Ebinger

Saravanan Vivekanandarajah Sathasivampillai[1,2]*(iD), Pholtan Rajamanoharan[3](iD)

[1] KnowledgeLink Group, Inc., Waltham, MA 02451, USA

[2] *Boigai Institute, Batticaloa 30000, Sri Lanka*

[3] *Provincial Herbal Garden Management Center, Trincomalee 31000, Sri Lanka*

Abstract: *Vachellia leucophloea* (Roxb.) Maslin, Seigler & Ebinger is a tree that fits into the *Fabaceae* family. *V. leucophloea* has been applied to heal including bronchitis, diabetes, high cholesterol, leprosy, and snakebite. Phytochemicals including betulinic acid-3-O-β-d-maltoside; Δ^7-avenasterol; leucophleol; leucophleoxol; and leucoxol; have been isolated from bark, root, and leaf of this plant species. This systematic review article purposes to evaluate, outline, and document the bioactivities associated with available researches involving *V. leucophloea*. PubMed, Semantic Scholar, Scopus, ScienceDirect, and Web of Science electronic records were employed to find the applicable available works from 1900 to June 2021. So far, *in vivo* and *in vitro* scientific evidence is presently existing for several bioactivities. To date, antidiabetic, antidiarrheal, antihyperlipidemic, antipyretic, wound healing, antibacterial, antidementia, antifungal, antiinflammatory, antioxidant, antiplatelet, and bronchorelaxant activities have been scientifically demonstrated for different parts of this plant species. Only an antidiabetic compound {(-)-Fisetinidol-(4α,8)-[(-)-fisetinidol-(4α,6)]-(+)-catechin} has been isolated from this plant species. Further *in vitro, in vivo,* and clinical studies of various traditional medicinal uses of *V. leucophloea* should be investigated as well as the bioactive compounds should be identified.

Keywords: *Vachellia leucophloea, Acacia leucophloea, Fabaceae,* bioactivity, antioxidant activity

1. Introduction

Vachellia leucophloea (Roxb.) Maslin, Seigler & Ebinger [synonyms: *Acacia leucophloea* (Roxb.) Willd. and *Mimosa leucophloea* Roxb.; Accepted Infraspecifics: *Vachellia leucophloea* var. *leucophloea* and *Vachellia leucophloea* var. *microcephala* (Kurz) Maslin, Seigler & Ebinger] is a tree that fits into the *Fabaceae* family. It is called வெள்வேல் (Velvel) in Tamil / Siddha Medicine; Arimanja, Arimedaka, Godhaa-skandha, Raamaka, Arimeda, Irimeda, and Vitakhadir in Ayurveda; Kath Safed, Guyaa Babuul, and Vilaayati Babuul in Unani; and Distiller's acacia in English. *V. leucophloea* is native to Asia (Sri Lanka, India, Vietnam, Bangladesh, Myanmar, Thailand, Indonesia, and Pakistan) and has been introduced into Africa (Mauritius and Tanzania) and South America (Trinidad-Tobago). This plant species is used to make chemical products, fiber, food (human and animal), drink (human and animal), medicine, and used for wood (Global Biodiversity Information Facility 2021; Kew Science 2021; Khare 2007). This plant species has been

applied to heal including bleedings, bronchitis, constipation, cough, dental cavity, diabetes, diarrhea, dysentery, fevers, gingivitis, high cholesterol, indigestion, leprosy, nausea, snakebite, sore throat, and wounds (Bhadoria and Gupta 1981; Khare 2007; Sathasivampillai et al. 2017, 2018, 2016, 2015; Suriyamoorthy et al. 2012). Phytochemicals including betulinic acid-3-O-β-d-maltoside; linoleic acid; oleic acid; γ-tocopherol; β-tocopherol; β-sitosterol; Δ^7-avenasterol; myricetin; quercetin; leucophleol; leucophleoxol; leucoxol; catechin; O-methyl epicatechin; gallic acid; leuco-fisetinidin; ferulic acid; and syringic acid have been isolated from bark, root, and leaf of *V. leucophloea* (Del Carmen Apreda Rojas et al. 2001; Mishra and Srivastava 1985; Saxena and Srivastava 1986; Sulaiman et al. 2016; Valsakumari and Sulochana 1991; Zia-Ul-Haq et al. 2013).

This systematic review article purposes to evaluate, outline, and document the bioactivities associated with available researches involving *V. leucophloea*. This article will be

advantageous for the scholars who are concerned to perform forthcoming bioactivities and phytochemical linked researches employing this plant species.

2. Materials and Methods

PubMed, Semantic Scholar, Scopus, ScienceDirect, and Web of Science electronic records were employed to find the applicable available works from 1900 to June 2021. "*Vachellia leucophloea*", "*Acacia leucophloea*", "*Mimosa leucophloea*", "*Vachellia leucophloea* var. *leucophloea*", and "*Vachellia leucophloea* var. *microcephala*" were applied as exploration terms, and only bioactivities interrelated to available works were taken into account in this research article.

3. Results and discussion

3.1. Reported bioactivities of various parts of *V. leucophloea*

Table 1 presents the Level of scientific evidence, bioactivity, part used, extract / fraction / compound, assay / model, dose / concentration, and reference of available bioactivities linked studies of *V. leucophloea*. So far, *in vivo* and *in vitro* scientific evidence is presently existing for several bioactivities. Though, more *in vitro* scientific evidence is available at the moment. To date, antidiabetic, antidiarrheal, antihyperlipidemic, antipyretic, wound healing, antibacterial, antidementia, antifungal, antiinflammatory, antioxidant, antiplatelet, and bronchorelaxant activities have been scientifically demonstrated for different parts of this plant species (Bobade 2020; Doss et al. 2012; Gupta et al. 2011, 2012; Imram et al. 2014; Imran et al. 2011, 2012; Jhade et al. 2012; Koppula and Koppula 2012; Madhavi et al. 2014; Shahid and Firdous 2012; Sowndhararajan et al. 2016; Sulaiman et al. 2013; Suriyamoorthy et al. 2012; Zia-Ul-Haq et al. 2013). Among these reported bioactivities, antibacterial and antioxidant activities have the most number of published works. Antidiabetic, antidiarrheal, antihyperlipidemic, antipyretic, and wound healing activities have only *in vivo* evidence, whereas, antibacterial, antidementia, antifungal, antiinflammatory, antioxidant, antiplatelet, and bronchorelaxant activities have only *in vitro* evidence. None of the reported bioactivity has both *in vitro* and *in vivo* evidence. Plant parts bark, flower, leaf, and root of *V. leucophloea* have been used to study various bioactivities. Anyway, bark has been used in the majority of the investigations. Thus far, only an antidiabetic compound {(-)-Fisetinidol-(4α,8)-[(-)-fisetinidol-(4α,6)]-(+)-catechin} has been isolated from this plant species (Ahmed et al. 2014). At the moment, traditional medicinal uses to treat such as bronchitis, diabetes, diarrhea, fevers, wounds, and high cholesterol have scientific evidence (Imram et al. 2014; Imran et al. 2011; Madhavi et al. 2014; Suriyamoorthy et al. 2012). On the other hand, other traditional medicinal treatments for constipation, dysentery, leprosy, nausea, and snakebite, have no scientific evidence at the moment. Only noteworthy

reported investigations which used the lowest concentration / dose used are deliberated in detail under.

3.2. Reported *in vivo* bioactivities
3.2.1. Antidiabetic activity

Ethanol extract prepared using bark was orally administered to Streptozotocin-Nicotinamide-induced diabetic rats at 200 mg/kg for 14 days. The results showed that there was a significant reduction in elevated blood glucose concentrations. Glibenclamide at a dose of 10 mg/kg was used as a standard drug in this study (Madhavi et al. 2014).

3.2.2. Antidiarrheal activity

In a study conducted by Imran et al. (2011), 100 mg/kg bark methanol (80%) extract was orally administered to castor oil-induced diarrheal mice. After one hour, it was observed that there was a protective property against diarrhea. Loperamide (10 mg/kg) was used aa a standard medication in this investigation (Imran et al. 2011).

3.2.3. Antihyperlipidemic activity

Bark ethanol extract (400 mg/kg) was orally administered to Streptozotocin-nicotinamide-induced diabetic rats for 14 days. It was noticed that there was a reduction in the increased triglycerides, total cholesterol, low-density lipoprotein cholesterol, and Very-low-density lipoprotein cholesterol levels. Glibenclamide at a dose of 10 mg/kg was used as a standard drug in this study (Madhavi et al. 2014).

3.2.4. Antipyretic activity

Antipyretic activity of methanol extract of bark (100 mg/kg) was studied in yeast-induced pyrexia mice. After 30 minutes, it was observed that the increased temperature of 38.24 °C was reduced to 37.97 °C. Paracetamol at a dose of 10 mg/kg was used as a standard drug in this study (Gupta et al. 2012).

3.2.5. Wound healing activity

Suriyamoorthy et al. (2012) investigated applied an ointment containing 2% of bark ethanol extract to excision and incision wounds in rats. It was detected that the wounds were contracted and there was a significant wound healing effect. Betadine ointment was employed as a standard medication in this investigation (Suriyamoorthy et al. 2012).

3.2. Reported *in vitro* bioactivities
3.2.1. Antibacterial activity

Leaf methanol extract at 25 mg/ml concentration revealed the antibacterial activity in the *Escherichia coli* assay. Ciprofloxacin was used as a positive control at 0.31 µg/ml concentration in this study (Gupta et al. 2011).

3.2.2. Antidementia activity

Sulaiman et al. (2013) researched the antidementia activity of ethanol (50%) extract in acetylcholinesterase inhibitory assay. Results exhibited that 1 mg/ml was an effective concentration in this research. Anyway, the authors did not state the plant part and the positive control used in this research (Sulaiman et al. 2013).

Table 1 Reported bioactivities of *V. leucophloea*

Level of scientific evidence	Bioactivity	Part used	Extract / compound	Assay / model	Dose / concentration	Reference
In vivo	Antidiabetic	Bark	Ethanol	Streptozotocin-Nicotinamide-induced diabetic	200 mg/kg	(Madhavi et al. 2014)
In vivo	Antidiarrheal	Bark	Methanol (80%)	Castor oil-induced diarrheal	100 mg/kg	(Imran et al. 2011)
In vivo	Antihyperlipidemic	Bark	Ethanol	Streptozotocin-nicotinamide-induced diabetic	400 mg/kg	(Madhavi et al. 2014)
In vivo	Antipyretic	Bark	Methanol	Yeast-induced pyrexia	100 mg/kg	(Gupta et al. 2012)
In vivo	Wound healing	Bark	Ethanol	Excision wound, Incision wound	2%	(Suriyamoorthy et al. 2012)
In vitro	Antibacterial	Bark	Aqueous, Methanol	*Bacillus subtilis, Escherichia coli, Klebseilla pneumonia, Proteus vulgaris, Pseudomonas florescence*	NS	(Koppula and Koppula 2012)
In vitro	Antibacterial	Flower	Methanol	*Bacillus subtilis*	8 mg	(Shahid and Firdous 2012)
In vitro	Antibacterial	Flower	Methanol	*Escherichia coli, Proteus mirabilis, Pseudomonas aeruginosa, Salmonella typhi, Staphylococcus aureus*	9 mg	(Shahid and Firdous 2012)
In vitro	Antibacterial	Leaf	Aqueous	*Staphylococcus aureus, Streptococcus agalactiae*	100 mg/ml	(Doss et al. 2012)
In vitro	Antibacterial	Leaf	Methanol	*Cutibacterium acnes, Escherichia coli, Salmonella typhi, Staphylococcus aureus*	NS	(Bobade 2020)
In vitro	Antibacterial	Leaf	Methanol	*Staphylococcus aureus*	100 mg/ml	(Doss et al. 2012)
In vitro	Antibacterial	Leaf	Methanol	*Streptococcus agalactiae*	200 mg/ml	
In vitro	Antibacterial	Leaf	Methanol	*Bacillus Subtilis, Pseudomonas aeruginosa*	75 mg/ml	(Gupta et al. 2011)
In vitro	Antibacterial	Leaf	Methanol	*Escherichia coli*	25 mg/ml	
In vitro	Antibacterial	Leaf	Methanol	*Staphylococcus aureus*	50 mg/ml	
In vitro	Antibacterial	Pod	Methanol	*Bacillus subtilis, Escherichia coli, Pseudomonas aeruginosa, Salmonella typhi, Staphylococcus aureus*	7 mg	(Shahid and Firdous 2012)
In vitro	Antibacterial	Pod	Methanol	*Proteus mirabilis*	6 mg	
In vitro	Antibacterial	Root	Methanol	*Bacillus subtilis, Escherichia coli, Proteus mirabilis, Pseudomonas aeruginosa, Salmonella typhi, Staphylococcus aureus*	13 mg	
In vitro	Antibacterial	Seed	Methanol	*Bacillus subtilis*	5 mg	

Level of scientific evidence	Bioactivity	Part used	Extract / compound	Assay / model	Dose / concentration	Reference
In vitro	Antibacterial	Seed	Methanol	*Escherichia coli, Proteus mirabilis, Pseudomonas aeruginosa, Salmonella typhi, Staphylococcus aureus*	6 mg	
In vitro	Antidementia	NS	Ethanol (50%)	Acetylcholinestrase inhibitory	1 mg/ml	(Sulaiman et al. 2013)
In vitro	Antidiabetic	Bark	(-)-Fisetinidol-(4α,8)-[(-)-fisetinidol-(4α,6)]-(+)-catechin	α-Glucosidase inhibitory	102.3 μM (IC$_{50}$)	(Ahmed et al. 2014)
In vitro	Antifungal	Flower	Methanol	*Aspergillus effusus, Aspergilus niger, Aspergilus parasiticus, Saccharomyces cerevisiae*	12 mg	(Shahid and Firdous 2012)
In vitro	Antifungal	Flower	Methanol	*Candida albicans*	11 mg	
In vitro	Antifungal	Flower	Methanol	*Fusarium solani*	9 mg	
In vitro	Antifungal	Pod	Methanol	*Aspergillus effusus, Aspergilus niger, Aspergilus parasiticus, Saccharomyces cerevisiae, Fusarium solani*	8 mg	
In vitro	Antifungal	Pod	Methanol	*Candida albicans*	7 mg	
In vitro	Antifungal	Root	Methanol	*Aspergillus effusus, Aspergilus niger, Aspergilus parasiticus, Candida albicans, Fusarium solani, Saccharomyces cerevisiae*	16 mg	
In vitro	Antifungal	Seed	Methanol	*Aspergillus effusus, Aspergilus niger, Aspergilus parasiticus, Fusarium solani*	9 mg	
In vitro	Antifungal	Seed	Methanol	*Candida albicans, Saccharomyces cerevisiae*	10 mg	
In vitro	Antiinflammatory	Bark	Acetone	Lipopolysaccharide-stimulated RAW 264.7 macrophage cell	25 μg/ml	(Sowndhararajan et al. 2016)
In vitro	Antioxidant	Bark	Methanol (80%)	Ferric reducing antioxidant power	2234.43 μmol/g	(Imram et al. 2014)
In vitro	Antioxidant	Bark	Methanol (80%)	Total radical-trapping antioxidant parameter	90.91 μmol/g	
In vitro	Antioxidant	Bark	Methanol (80%)	Trolox equivalent antioxidant capacity	682.95 μmol/g	
In vitro	Antioxidant	Leaf	Methanol	DPPH free radical scavenging	1000 μg/ml	(Bobade 2020)
In vitro	Antioxidant	Leaf	Methanol (80%)	Ferric reducing antioxidant power	233.17 μmol/g	(Zia-Ul-Haq et al. 2013)
In vitro	Antioxidant	Leaf	Methanol (80%)	Total radical-trapping antioxidant parameter	68.39 μmol/g	
In vitro	Antioxidant	Leaf	Methanol (80%)	Trolox equivalent antioxidant capacity	543.03 μmol/g	

Level of scientific evidence	Bioactivity	Part used	Extract / compound	Assay / model	Dose / concentration	Reference
In vitro	Antioxidant	NS	Ethanol (50%)	ABTS radical scavenging	0.36 mmol/l	(Sulaiman et al. 2013)
In vitro	Antioxidant	NS	Ethanol (50%)	DPPH free radical scavenging	18.38 μg/ml (EC$_{50}$)	
In vitro	Antioxidant	NS	Ethanol (50%)	Nitric Oxide quenching capacity	10 μg	
In vitro	Antioxidant	Pod	Methanol (80%)	Ferric reducing antioxidant power	254.42 μmol/g	(Zia-Ul-Haq et al. 2013)
In vitro	Antioxidant	Pod	Methanol (80%)	Total radical-trapping antioxidant parameter	76.02 μmol/g	
In vitro	Antioxidant	Pod	Methanol (80%)	Trolox equivalent antioxidant capacity	683.23 μmol/g	
In vitro	Antioxidant	Root	Aqueous, Ethanol, Petroleum ether	Superoxide radical scavenging	50 μg/ml	(Jhade et al. 2012)
In vitro	Antioxidant	Seed	Methanol (80%)	Ferric reducing antioxidant power	178.14 μmol/g	(Zia-Ul-Haq et al. 2013)
In vitro	Antioxidant	Seed	Methanol (80%)	Total radical-trapping antioxidant parameter	49.14 μmol/g	
In vitro	Antioxidant	Seed	Methanol (80%)	Trolox equivalent antioxidant capacity	529.66 μmol/g	
In vitro	Antiplatelet	Bark	Methanol	Adenosine 5' diphosphate-induced human platelet	0.83 mg/ml (IC$_{50}$)	(Imran et al. 2012)
In vitro	Bronchorelaxant	Bark	Methanol (80%)	Guinea pig ileum	0.3 mg/ml	(Imran et al. 2011)
In vitro	Bronchorelaxant	Bark	Methanol (80%)	Isolated rabbit jejunum	0.1 mg/ml	(Imran et al. 2011)

Abbreviation:
ABTS: (3-ethylbenzothiazoline-6-sulphonic acid); DPPH: 2,2-diphenyl-1-picrylhydrazyl; EC$_{50}$: Half maximal effective concentration; FRAP: Ferric Reducing Antioxidant Power; IC$_{50}$: Half maximal inhibitory concentration; NS: Not Stated

3.2.3. Antifungal activity
Methanol extract of the pod (7 mg) showed the antifungal activity in the *Candida albicans* assay. Both Itraconazole (2 mg) and Amphotericin B (2 mg) were applied as a positive control in this investigation (Shahid and Firdous 2012).

3.2.4. Antiinflammatory activity
Acetone was used to prepare the extract of bark and antiinflammatory activity was studied in the lipopolysaccharide-stimulated RAW 264.7 macrophage cell line. Outcomes revealed that 25 μg/ml was the effective concentration in this study (Sowndhararajan et al. 2016).

3.2.5. Antioxidant activity
An investigation carried out by Jhade et al. (2012) unveiled that aqueous, ethanol, and petroleum ether extracts of root at 50 μg/ml concentration showed antioxidant activities in superoxide radical scavenging assay. Ascorbic acid was employed as a standard drug in this investigation. However, the authors did not mention the concentration of the standard drug used in this investigation (Jhade et al. 2012).

3.2.6. Antiplatelet activity
Bark methanol extract at IC$_{50}$ of 0.83 mg/ml exhibited antiplatelet activity in adenosine 5' diphosphate-induced human platelet assay. Besides, the authors did not mention the name and concentration of the standard drug used in this research (Imran et al. 2012).

3.2.7. Bronchorelaxant activity

Imran et al. (2011) revealed the bronchorelaxant activity of bark methanol (80%) extract in isolated rabbit jejunum assay at a concentration of 0.1 mg/ml. Both Nifedipine and Dicyclomine were applied as positive controls in this study. Again, the authors did not state the concentration of the positive control used in this study (Imran et al. 2011).

4. Conclusion

V. leucophloea has a great number of traditional medicinal uses although, only some of these utilizations have scientific evidence at the moment. Therefore, further *in vitro, in vivo*, and clinical studies of various traditional medicinal uses of this plant species should be investigated as well as the bioactive compounds should be identified. The reaction mechanism of the bioactive extracts and bioactive compounds of this plant species also should be further studied in detail. These bioactive compounds might be lead compound candidates in future drug discovery programs. This systematic review article evaluated, outlined, and documented the bioactivities associated with available researches involving *V. leucophloea*.

Acknowledgments

Authors' contributions: Both authors contributed equally to this work.

Conflict of interest

The authors declare that there is no conflict of interest.

References

Ahmed, S, Lin, HC, Nizam, I, Khan, NA, Lee, SS, Khan, NU (2014) A Trimeric Proanthocyanidin from the Bark of *Acacia leucophloea* Willd. Rec Nat Prod 8:294–298

Bhadoria, BK, Gupta, RK (1981) A note on hydrocyanic acid content in Acacia leucophloea Roxb. Willd. Curr Sci 50:689–690.

Bobade, AF (2020) GC-MS and Pharmacognostic Study of *Acacia Leucophloea* leaves. Int J Pharma Bio Sci 11:1–9

Del Carmen Apreda Rojas, M, Cano, FH, Rodríguez, B (2001) Diterpenoids from *Acacia leucophloea*: Revision of the structures of leucophleol and leucophleoxol. J Nat Prod 64: 899–902. doi: https://doi.org/10.1021/np010145z

Doss, A, Mubarack, HM, Vijayasanthi, M, Venkataswamy, R (2012) *In vitro* antibacterial activity of certain wild medicinal plants against bovine mastitis isolated contagious pathogens. Asian J Pharm Clin Res 5:90–93

Global Biodiversity Information Facility (2021) *Vachellia leucophloea* (Roxb.) Maslin, Seigler & Ebinger. https://www.gbif.org/species/7769517. Accessed 31 May 2021

Gupta, R, Gupta, AK, Singla, RK, Aiswarya, G (2011) Preliminary investigation of antimicrobial property of *Acacia leucophloea* leaves extract. Int J Phytomedicine 3:308–311

Gupta, R, Kumar, A, Aiswarya, G, Singh, J (2012) Antipyretic activity of methanol extract of *Acacia leucophloea* Roxb bark. Int J Plant Animal Env Sci 2:138–140

Imram, I, Zia-Ul-Haq, M, Calani, L., Mazzeo, T, Pellegrini, N (2014) Phenolic profile and antioxidant potential of selected plants of Pakistan. J Appl Bot Food Qual 87:30–35

Imran, I, Hussain, L, Ahmed, S, Rasool, N, Rasool, S, Abbas, G, Ali, MY (2012) Antiplatelet activity of methanolic extract of *Acacia leucophloea* bark. J Med Plant Res 6:4185–4188

Imran, I, Hussain, L, Zia-Ul-Haq, M, Janbaz, KH, Gilani, AH, De Feo, V (2011) Gastrointestial and respiratory activities of *Acacia leucophloea*. J Ethnopharmacol 138:676–682

Jhade, D, Jain, S, Jain, A, Sharma, P (2012) Pharmacognostic Screening, Phytochemical Evaluation and *in vitro* free radical Scavenging Activity of *Acacia leucophloea* Root. Asian Pac. J. Trop. Biomed. 2:S501–S505

Kew Science (2021) *Vachellia leucophloea* (Roxb.) Maslin, Seigler & Ebinger. Plants of the World Online. http://powo.science.kew.org/taxon/urn:lsid:ipni.org:names:771 32539-1. Accessed 31 May 2021

Khare, CP (2007) *Acacia leucophloea* Willd., In: Indian Medicinal Plants: An Illustrated Dictionary. Springer, New York

Koppula, US, Koppula, S (2012) Antibacterial activity of some selected Indian medicinal plant barks. Int J Bio-Pharm Res 1:30–33

Madhavi, M, Kiran, S, Ramesh, D (2014) Evaluation of antidiabetic, antihyperlipidemic and antioxidant activities of *Acacia leucophloea* in streptozotocin-nicotinamide induced type II diabetic in rats. Glob J Pharmacol 8:64–72. doi: https://doi.org/10.5829/idosi.gjp.2014.8.1.81218

Mishra, M, Srivastava, SK (1985) Betulinic acid-3-O-β-d-maltoside from *Acacia leucophloea* Wild. Indian J Pharm Sci 47:154–155

Perales, A, Martínez-Ripoll, M, Fayos, J, Bansal, RK, Joshi, KC, Patni, R, Rodríguez, B (1980) Leucoxol, a new diterpenoid from *Acacia leucophloea*. X-ray structure determination. Tetrahedron Lett 21:2843–2844. doi: https://doi.org/10.1016/S0040-4039(00)78623-0

Sathasivampillai, S, Rajamanoharan, P, Munday, M, Heinrich, M (2017) Plants currently used to treat diabetes in Sri Lankan Siddha Medicine – an ethnobotanical survey in the Eastern Province. In: World Congress Integrative Medicine & Health 2017: Part three, Springer Nature, Berlin, 3–5 May 2017

Sathasivampillai, SV, Rajamanoharan, PR, Heinrich, M, Munday, M (2015) Preparations and plants used to treat diabetes in Sri Lankan Siddha Medicine. In: 3rd International Conference on Ayurveda, Unani, Siddha and Traditional Medicine, Institute of Indigenous Medicine, University of Colombo, Colombo, 11-13 December 2015

Sathasivampillai, SV, Rajamanoharan, PRS, Heinrich, M (2018) Siddha Medicine in Eastern Sri Lanka Today–Continuity and

Change in the Treatment of Diabetes. Front Pharmacol 9. doi: https://doi.org/10.3389/fphar.2018.01022

Sathasivampillai, SV, Rajamanoharan, PRS, Munday, M, Heinrich, M (2016) Plants used to treat diabetes in Sri Lankan Siddha Medicine – An ethnopharmacological review of historical and modern sources. J Ethnopharmacol 198:531–599. doi: https://doi.org/10.1016/j.jep.2016.07.053

Saxena, M, Srivastava, SK (1986) Anthraquinones from the roots of *Acacia leucophloea*. J Nat Prod 49:205–209

Shahid, SA, Firdous, N (2012) Antimicrobial screening of *Albizia lebbeck* (l.) Benth. and *Acacia leucophloea* (Roxb.). Afr J Pharm Pharmacol 6:3180–3183

Sowndhararajan, K, Santhanam, R, Hong, S, Jhoo, JW, Kim, S (2016) Suppressive effects of acetone extract from the stem bark of three *Acacia* species on nitric oxide production in lipopolysaccharide-stimulated RAW 264.7 macrophage cells. Asian Pac J Trop Biomed 6:658–664

Sulaiman, CT, Nasiya, KK, Balachandran, I (2016) Isolation and mass spectroscopic characterization of phytochemicals from the bark of *Acacia leucophloea* (Roxb.) Willd. Spectrosc Lett 49:391–395

Sulaiman, CT, Sadashiva, CT, George, S, Goplakrishnan, VK, Balachandran, I (2013) Chromatographic studies and *in vitro* screening for acetyl cholinesterase inhibition and antioxidant activity of three *Acacia* species from South India. Anal Chem Lett 3:111–118

Suriyamoorthy, S, Subramaniam, K, Wahab, F, Karthikeyan, G (2012) Evaluation of wound healing activity of *Acacia leucophloea* bark in rats. Rev Bras Farmacogn 22:1338–1343

Valsakumari, MK, Sulochana, N (1991) Chemical examination of *Acacia leucophloea* Willd.   J Indian Chem Soc 68:673–674

Zia-Ul-Haq, M, Ćavar, S, Qayum, M, Khan, I, Ahmad, S (2013) Chemical composition and antioxidant potential of *Acacia leucophloea* Roxb. Acta Bot Croat 72;133–144